HHS Public Access
Author manuscript
J Innate Immun. Author manuscript; available in PMC 2015 June 06.

Published in final edited form as:
J Innate Immun. 2014 ; 6(6): 831–845. doi:10.1159/000363338.

Porphyromonas gingivalis fimbriae dampen P2X7-dependent IL-1β secretion

Ana Carolina Morandini[a,b,1], **Erivan S. Ramos-Junior**[a,1], **Jan Potempa**[c], **Ky-Anh Nguyen**[d], **Ana Carolina Oliveira**[a], **Maria Bellio**[e], **David M. Ojcius**[f], **Julio Scharfstein**[a], and **Robson Coutinho-Silva**[a,b]

[a]Programa de Imunobiologia, Instituto de Biofísica Carlos Chagas Filho, Universidade Federal do Rio de Janeiro, Rio de Janeiro, RJ, Brasil [b]Instituto Nacional de Ciência e Tecnologia para Pesquisa Translacional em Saúde e Ambiente na Região Amazônica (INPeTAm/UFRJ) [c]Oral Health and Systemic Diseases Research Group, University of Louisville School of Dentistry, Louisville, KY 40202, USA and Department of Microbiology, Faculty of Biochemistry, Biophysics and Biotechnology, Jagiellonian University, Krakow, Poland [d]Faculty of Dentistry, University of Sydney, Sydney, NSW 2006, Australia [e]Departmento de Imunologia, Instituto de Microbiologia Paulo de Góes, Universidade Federal do Rio de Janeiro, Rio de Janeiro, Brazil [f]Department of Molecular Cell Biology and Health Sciences Research Institute, University of California, Merced, CA, USA

Abstract

Porphyromonas gingivalis is a major contributor to the pathogenesis of periodontitis, an infection-driven inflammatory disease that leads to bone destruction. This pathogen stimulates pro-IL-1β synthesis but not mature IL-1β secretion, unless the P2X7 receptor is activated by extracellular ATP. Here, we investigated the role of *Pg* fimbriae in eATP-induced IL-1β release. Bone marrow derived macrophages (BMDMs) from wild type (WT) or P2X7-deficient mice were infected with *Pg* (strain 381) or isogenic fimbriae deficient (strain DPG3) with or without subsequent eATP stimulation. DPG3 induced higher IL-1β secretion after eATP stimulation compared to 381 in WT BMDMs, but not in P2X7-deficient cells. This mechanism was dependent of K^+ efflux and Ca^{2+}-iPLA$_2$ activity. Accordingly, non-fimbriated *Pg* failed to inhibit apoptosis via eATP/P2X7-pathway. Furthermore, *Pg*-driven stimulation of IL-1β was TLR2- and MyD88-dependent, and irrespective of fimbriae expression. Fimbriae-dependent down-modulation of IL-1β was selective, as levels of other cytokines remained unaffected by P2X7 deficiency. Confocal microscopy demonstrated the presence of discrete P2X7 expression in the absence of *Pg* stimulation which was enhanced by 381-stimulated cells. Notably, DPG3-infected macrophages revealed a distinct pattern of P2X7 receptor expression with a markedly foci formation. Collectively, these data

Corresponding author: Robson Coutinho-Silva, Instituto de Biofisica Carlos Chagas Filho – UFRJ, Edifício do Centro de Ciências da Saúde, Bloco G., Av. Carlos Chagas Filho, 373, Cidade Universitária, Ilha do Fundão, Rio de Janeiro, RJ, 21941-902 – Brazil Phone: +55 21 2562 6565, Fax. +55 21 2280 8193, rcsilva@biof.ufrj.br.
[1]A.C.M. and E.S.R.J. contributed equally to this work

Disclosure Statement
The authors have no financial conflicts of interest.

demonstrate that eATP-induced IL-1β secretion is impaired by *Pg* fimbriae in a P2X7-dependent manner.

Keywords

Porphyromonas gingivalis; P2X7 receptor; IL-1β; macrophage

Introduction

The pro-inflammatory cytokine interleukin (IL)-1β is a key mediator in the host immune response against infection as it plays a large role in the initiation and maintenance of the inflammatory response elicited by pathogens. IL-1β is synthesized as an inactive precursor, pro-IL-1β, in the cytosol of monocytes, macrophages and epithelial cells. Recognition of pathogen associated molecular patterns (PAMPs) by pattern recognition receptors (PRRs) is generally described as a first step that leads to synthesis of pro-IL-1β but is not sufficient for secretion. The infected cell must be stimulated with a second signal which can be released from infected cells or other stressed cells, called damage-associated molecular patterns (DAMPs) [1]. Pro-IL-1β is then proteolytically cleaved into the 17 kDa biologically active form [2] and can be released into the extracellular space through a variety of secretory mechanisms present in monocytes and macrophages [1,3–5]. Activation of caspase-1, which is responsible for IL-1β processing, is regulated by a multi-protein complex called the inflammasome [6,7].

As a consequence, many pathogens have evolved different mechanisms to subvert IL-1β production, including the inhibition of inflammasome activation at different levels of the signaling cascade [8]. Recent studies suggest that pathogen-derived inflammasome inhibitors range from caspase inhibitors (serpins) to pore-forming toxins, suggesting that the mechanisms that have evolved to perturb the inflammasome are widespread [9].

Porphyromonas gingivalis is among the major contributors to the pathogenesis of periodontitis – an infectious and inflammatory disease that can lead to the destruction of tooth-supporting structures, including alveolar bone. It also acts as a keystone pathogen in the pathogenesis of this inflammatory disease since its presence in low numbers is sufficient to shift the subgingival microbiota on the tooth surface to a disease-associated consortium [10]. In this context, *P. gingivalis* expresses a number of virulence factors to acquire essential nutrients for growth and to evade the host immune system. Prominent virulence factors include cysteine proteinases called gingipains, which degrade chemokines, limiting trans-endothelial migration of leukocytes to the infection foci [11] and playing an important role in pathogenesis by degrading / shedding receptors and cytokines essential for phagocyte function as reviewed elsewhere [12].

While studying the first signal driving IL-1β production in *P. gingivalis*-infected macrophages, Papadopoulos *et al.* observed that fimbriae subvert innate immunity via activation of TLR2 [13]. There is evidence that *P. gingivalis* by itself is not a potent inducer of IL-1β secretion, since gingival epithelial cells infected with *P. gingivalis* secrete IL-1β only if the cells are subsequently stimulated with extracellular ATP (eATP), a well-known danger signal released from injured, dying or activated cells [14]. Binding of eATP to P2X7 causes the formation of a non-selective pore which results in K^+ efflux [15], which in turn acts as a second signal that can result in NLRP3 inflammasome activation [16]. In this context, it was recently demonstrated that *P. gingivalis* suppresses inflammasome activation in polymicrobial cultures via a mechanism involving the blockade of endocytosis [17]. Interestingly, *P. gingivalis* LPS by itself is not sufficient to inhibit inflammasomes, suggesting that the pathogen subverts immunity by mobilizing additional virulence factors [18]. To the best of our knowledge, this is the first study to demonstrate that fimbriae can impair eATP-induced IL-1β secretion by acting at the level of the P2X7 receptor.

Material and Methods

Mice

$TLR2^{-/-}$, $TLR4^{-/-}$ and $MyD88^{-/-}$ mice were used in this work as previously described [19]. C57BL/6 mice, and $P2X7^{-/-}$ receptor mice (originally from the Jackson Laboratory, USA) were bred at the Animal House of Transgenic Mice of Federal University of Rio de Janeiro. This study was approved by the Ethics Committee of the Instituto de Biofísica Carlos Chagas Filho (CEUA- UFRJ) under number IBCCF 154.

Bacteria

Frozen stocks of WT *P. gingivalis* strain 381 and the major fimbriae mutant (DPG3) were previously described [20] and were grown anaerobically at 37°C on blood agar plates for 5 days as described [21]. Plate-grown organisms were used to inoculate liquid cultures of brain heart infusion broth (BD Biosciences) supplemented with yeast extract (0.5%; Sigma-Aldrich), hemin (10 μg/ml; Sigma-Aldrich), and menadione (1 μg/ml; Sigma-Aldrich). Erythromycin (5μg/ml) was used to maintain the DPG3 fimbriae mutant. Liquid cultures were grown anaerobically for 18–24 h and harvested at mid- to late-log phase. Cells were washed twice in PBS before use.

Fimbriae

Fimbriae (Fim) from WT *P. gingivalis* were purified according to a method described previously [21,22]. Briefly, *P. gingivalis* Fim were purified from the supernatant of centrifuged bacteria by ammonium sulfate precipitation and chromatography on a DEAE-Sepharose CL-6B column. SDS-PAGE analysis of the final preparation showed minor and major protein bands of 67 kDa (Mfa1) and 41 kDa (FimA) (data not shown), respectively, indicating that a mixture of major (FimA) and minor (Mfa1) Fim was obtained. The fimbrial preparations tested negative for endotoxin (<6 endotoxin U/mg protein), according to a quantitative Limulus amebocyte lysate assay (BioWhittaker).

Reagents

RPMI 1640, penicillin/streptomycin solution, and sodium pyruvate were purchased from Invitrogen, Life Technologies. FBS was purchased from Gibco, Life Technologies. ATP, murine IL-1β Ab, murine β-actin Ab were purchased from Sigma Aldrich. Antibodies for p-BAD, p-STAT3 and STAT3 were purchased from Cell Signalling. Alexa Fluor 488 anti-mouse CD11b and APC anti-mouse F4/80 were purchased from Biolegend. P2X7 Ab was from Alomone. Fluorochrome-conjugated secondary Ab linked to Alexa Fluor 488 was from Life Technologies. Caspase-1 Ab was purchased from Santa Cruz Biotechnology. BEL was from Cayman Chemical.

Bone marrow-derived macrophages (BMDMs)

Fresh bone marrow cells were used to generate BMDMs, using L929-cell conditioned medium (LCCM) as a source of macrophage colony stimulating factor [23]. Cells were resuspended in 10 ml bone marrow differentiation media (R20/30; composition: RPMI1640 supplemented with 20% fetal bovine serum, 30% LCCM, 100 U/ml penicillin, 100 mg/ml streptomycin and 1 mM sodium pyruvate) and were seeded in untreated 90×15 mm culture dishes and incubated at 37°C in a 5% CO_2 atmosphere. Three days after seeding, an extra 10 ml of fresh R20/30 were added per dish and incubated for additional 3 days. On day 6, the attached cells were washed and detached with 10 ml of cold sterile PBS. Cells were centrifuged at 200 × g for 5 minutes and resuspended in 10 ml of BMDM cultivation media (R10/5; composition: RPMI 1640, 10% fetal bovine serum, 5% LCCM). Cells were seeded at a density of 10^6/ml on the day before the experiments. The macrophage purity of these preparations was usually >95% as assessed by flow cytometry using murine macrophage antibody Alexa Fluor 488 anti-CD11b and APC anti- F4/80 (Biolegend). For infection with *P.gingivalis*, a multiplicity of infection (MOI) of 100 was used for all the experiments as described in the figure legends.

Total RNA extraction and RT-qPCR

Total RNA was extracted from BMDMs (10^6/ml) using Trizol reagent following manufacturer's recommendations. For cDNA synthesis, 1 μg of RNA, oligo(dT), random primers, nuclease-free water, and a kit containing reverse transcriptase were used (Life Technologies). The quantitative polymerase chain reaction (qPCR) was performed with the SYBR-green fluorescence quantification system, and the PCR cycling parameters were 95 °C (10 min), and then 40 cycles of 95 °C (30 sec), 60 °C (1 min), followed by the standard denaturation curve. Primer sets were as follows: *IL-1b* forward, 5′-TTCAGGCAGGCAGTATCACTC; *IL-1b* reverse, 5′-CCACGGGAAAGACACAGGTAG; *P2rx7* forward, 5′-AATCGGTGTGTTTCCTTTGG; *P2rx7* reverse, 5′-CCGGGTGACTTTGTTTGTCT; *Gapdh* forward, 5′-GGTCATCCCAGAGCTGAACG; *Gapdh* reverse, 5′-TTGCTGTTGAAGTCGCAGGA; IL-1b and P2rx7 to *gapdh* relative expression was calculated using the comparative cycle threshold (Ct) method and normalized to the level of unstimulated BMDMs.

ELISA

Mouse IL-1β, TNF-α, IL-6, IL-10, CXCL1/KC in culture supernatant were measured by ELISA kits (R&D Systems) after 6 h or 18 h of *P. gingivalis* stimulation followed by 30 min incubation with 5 mM eATP, according to the legends of each figure. Assays were performed in triplicate for each independent experiment.

Cells extracts and Western Blot

Cells were lysed in ice-cold Cell-lytic solution (Sigma-Aldrich) containing 1% of a complete protease and phosphatase inhibitor mixture (Sigma-Aldrich). Mature IL-1β in the culture supernatant was precipitated by 20% trichloroacetic acid. Protein samples (20–50μg of protein) were separated by 12% SDS-PAGE and transferred to Immobilion polyvinylidene difluoride membranes (Millipore) by electroblotting (Bio-Rad), and then probed with respective antibodies. Protein bands were visualized with the use of the West Pico Super Signal chemiluminescent substrate (Thermo Scientific), and exposed to a negative film, developed, and fixed. The same membranes were stripped and re-probed using β-actin (Sigma-Aldrich) as an internal control.

Flow cytometry

For apoptosis assays using annexin V and propidium iodide, BMDMs were washed twice with cold PBS and then stained with Alexa 488-conjugated annexin V and PI for 15 min at room temperature in Annexin V binding buffer using a Cell death/apoptosis Kit (Life technologies), according to manufacturer's instructions. Cells were analyzed on a FACS Calibur (BD Biosciences) with CellQuest software (BD Biosciences). Data are expressed as the percentage of positive cells for annexin V and propidium iodide as described in figure legends. Percentages of early apoptotic cells (Annexin V+/PI−) derived from WT BMDMs after 18 h of infection with *P. gingivalis* strains 381 or DPG3, or DPG3 infection and Fim stimulation (MOI of 100) followed by 5 mM eATP incubation for 30 min and stained for annexin V/PI, were normalized with respect to the value for Medium+5 mM ATP as previously described [24].

Lactate dehydrogenase (LDH) -based cytotoxicity assay

To measure plasma membrane integrity, we assayed serum lactate dehydrogenase (LDH) levels and calculated percentages of LDH release into the medium. LDH activity was measured spectrophotometrically using a commercial kit (Doles). After BMDMs were stimulated with each strain of *P. gingivalis* for 18h and an additional incubation for 30 min with or without 5mM eATP, the supernatants were transferred to an enzymatic assay plate and LDH substrate plus ferric alum were added to the wells and incubated in the dark for 3 minutes at 37°C. Subsequently, NAD was added and incubated for 6 minutes at 37°C, protected from light. The reaction was stopped with the stop solution provided with the kit and the absorbance was recorded at 490 nm using a microELISA plate reader (Thermo Scientific). The percentage of LDH release was calculated as ([LDH] sample/total [LDH]) ×100. [LDH] sample was the LDH level of the sample (released in medium) subtracted from the medium background (blank), and total [LDH] was the LDH content in the positive control well after addition of lysis solution (Triton 0.9%).

Imunofluorescence and confocal microscopy

For immunofluorescence, BMDMs were seeded at 10^5 cells/chamber in a 8-well glass LabTek (Nunc, Thermo Scientific, Illkirch, France). Then, the 8-well chambers were washed in PBS, fixed in fresh 4% paraformaldehyde for 15 min at room temperature, washed three times in PBS, for 5 min each time, permeabilized with 0.1% Triton X-100, for

30 min, and blocked by incubation with 3% bovine serum albumine in PBS for 30 min. The chambers were incubated overnight at 4°C with anti-P2X7 antibody (Alomone). After washing three times in PBS with 0.1% Triton X-100, for 5 min each time, they were incubated with fluorochrome-conjugated secondary antibody (linked to Alexa Fluor 488, Life Technologies). This and all subsequent steps were performed with minimal exposure of samples to light. Coverslips were mounted by using Vectashield Mounting Medium supplemented with DAPI (Vector Laboratories). The slides were viewed with a Leica TCS SP5 laser scanning confocal microscope by using the LAS AF software.

Statistics

Data were evaluated by one-way ANOVA with Tukey's post-test using GraphPad Prism v5. Where appropriate (comparison of two groups only), two-tailed t tests were also performed. Statistical differences were considered significant at the level of $p < 0.05$.

Results

Pg fimbriae impair IL-1β secretion only after eATP stimulation and this is dependent of K^+ efflux and phospholipase activity

We initially investigated the effect of *P. gingivalis* fimbriae on IL-1β release from BMDMs through stimulation with both WT (strain 381) and the isogenic fimbriae-deficient *P. gingivalis* (strain DPG3). Because IL-1β production requires two signals, we also investigated the influence of eATP on IL-1β release from BMDMs. For this, we quantified the release of IL-1β after 6h of infection followed by 30 min of eATP stimulation and compared to a control that was not treated with eATP (Fig. 1a). In the absence of eATP, low levels of IL-1β release were detected for wild-type *P.gingivalis* 381-stimulated cells. In contrast, IL-1β was barely detectable in conditioned media of DPG3-stimulated cells (Fig. 1a). However, in the presence of eATP, challenge with the non-fimbriated *P. gingivalis* mutant DPG3 elicited greater IL-1β secretion as compared to the wild-type 381 strain. To investigate if this was caused by a difference in the levels of pro-IL-1β, we performed Western blot of whole cell lysates (Fig. 1b). In the absence of eATP, pro-IL-1β expression was similar in 381- and DPG3-stimulated cells, but a significant quantity of mature IL-1β (17kDa) was detected only in the lysate of DPG3-stimulated macrophages. Interestingly, a substantial decrease in pro-IL-1β (33kDa) in DPG3-stimulated cells compared to 381 with eATP was detected, with no expression of the mature form in the lysate (Fig. 1b). When supernatants of the same samples were analyzed by Western blot, no detectable levels of IL-1β were found for BMDMs without ATP. Conversely, in the presence of eATP, DPG3-stimulated cells exhibited higher expression of both pro-IL-1β and mature IL-1β compared to 381-stimulated cells, corroborating the ELISA findings (Fig. 1b). We then compared the mRNA expression in BMDMs stimulated with both strains, 381 and DPG3, at different time points. At the transcriptional level, *P. gingivalis* 381 induced higher pro-IL-1β mRNA expression in BMDMs compared with DPG3 during the first 2 h and 4 h post-challenge (Fig. 1c). In contrast, BMDMs expressed more IL-1β mRNA when stimulated with DPG3 after 6 h (Fig. 1c).

To gain insight into the mechanism of IL-1β processing and because this has been shown to be dependent of K^+ efflux[25,26], we compared IL-1β processing and secretion between 381 and DPG3-stimulated cells in the presence of KCl (Figs. 1d and 1e). The increased extracellular KCl concentration significantly reduced *P. gingivalis*– induced IL-1β release by both strains (Figs. 1d and 1e). Finally, as eATP induces a non-classical IL-1β secretion involving microvesicles and exosomes and because it has been demonstrated that the fusion of secretory lysosomes with the plasma membrane can be regulated by Ca^{2+}-independent phospholipase A_2 (iPLA$_2$) activity [27], we investigated whether eATP-stimulated IL-1β release would be blocked by BEL (iPLA2 inhibitior) (Figs 1f and 1g). We found that BEL inhibited eATP-induced IL-1β processing and secretion (Figs 1f and 1g) which further emphasizes the role of phospholipase A_2 in the non-classical secretory events induced by eATP stimulation.

The P2X7 receptor is required for fimbriae-mediated inhibition of IL-1β secretion

We then evaluated the role of the P2X7 receptor in BMDMs infected with both strains of *P. gingivalis* (381 and DPG3). To this end, we used a third group of cells, stimulated with DPG3 plus fimbriae (10 μg/ml) to determine whether the supplementation with purified fimbriae would rescue original IL-1β response elicited by fimbriated *P. gingivalis* strain 381. We compared P2X7 mRNA expression after 2 h of infection (Fig. 2a), and protein P2X7 expression after 18 h of infection, followed by 30 min with or without eATP stimulation (Fig. 2b). We observed higher P2X7 mRNA expression in DPG3-stimulated cells as compared to 381 or the fimbriae-supplemented group (DPG3+Fim) (Fig. 2a). We found a discrete increase in P2X7 protein expression in *P. gingivalis*-stimulated cells, but there was no difference between 381- or DPG3-stimulated cells, with or without eATP (Fig. 2b). To test whether fimbriae-mediated inhibition of IL-1β secretion was dependent on signaling via the P2X7 receptor, we used BMDMs from P2X7$^{-/-}$ mice in a parallel study. Analysis of pro-IL-1β mRNA expression by qPCR showed no differences between mRNA levels from BMDMs derived from WT or P2X7$^{-/-}$ mice stimulated with *P. gingivalis* strains 381, DPG3 or DPG3+Fim (Fig. 2c). On the other hand, IL-1β secretion was significantly decreased in BMDMs derived from P2X7$^{-/-}$ mice as compared to WT (Fig. 2d). Additionally, there was no fimbriae-dependent inhibition of IL-1β secretion in BMDMs from P2X7$^{-/-}$ mice, linking P2X7 signaling pathway to fimbriae-regulated IL-1β secretion (Fig. 2d).

The P2X7 receptor is dispensable for *P. gingivalis*-induced TNF-α, IL-10, CXCL1 and IL-6 secretion

We next evaluated the profile of cytokines produced during *P. gingivalis* stimulation by comparing BMDMs derived from WT and P2X7$^{-/-}$ mice. Other cytokines such as TNF-α, IL-10, CXCL1 and IL-6 were produced when cells were challenged with wild-type *P. gingivalis* for 18 h followed by eATP (5mM) for 30 min (Fig. 3). The results were similar when the experiment was performed without eATP as a second signal (data not shown). This effect was induced by *P. gingivalis* fimbriae as the fimbriae-deficient strain, DPG3, failed to elicit a similar response, and there was recovery of cytokine production in the group with supplemented fimbriae. Furthermore, comparison of the WT and P2X7$^{-/-}$ BMDMs indicated that secretion of TNF-α, IL-10, CXCL1 and IL-6 was independent of the P2X7 receptor (Fig. 3). Collectively, these results indicate that, unlike IL-1β secretion, the profile of production of others cytokines, secreted in a canonical secretory pathway, was not altered in the absence of P2X7 receptor.

Fimbriae reduce pro-IL-1β processing mediated through P2X7 receptor activation

We compared the kinetics of pro-IL-1β conversion to its mature form in both whole cell extracts and supernatants from WT and P2X7$^{-/-}$ BMDMs. Within 1 h of infection, both cell extracts from WT and P2X7$^{-/-}$ showed an increase in pro-IL-1β (33kDa) levels when stimulated with *P. gingivalis* strain 381 (Fig. 4a). This is in contrast with cells stimulated with DPG3, where no expression of pro-IL-1β could be detected (Fig. 4a). Following stimulation for 2 h and 4 h, DPG3-stimulated macrophages produced pro-IL-1β but at lower levels, as compared with 381-stimulated cells (Fig. 4a). Interestingly, after 18 h of stimulation and in the absence of eATP, pro-IL-1β levels were similar between 381- and DPG3-stimulated cells, both in WT and P2X7$^{-/-}$ cells (Figs. 4b, 4c). However, following eATP addition, pro-IL-1β processing was higher in DPG3-compared with 381-stimulated cells, i.e. there was a decrease of pro- IL-1β in WT cell extracts (Fig 4b) but not in P2X7$^{-/-}$ extracts (Fig 4c). There were higher levels of the mature form (17kDa) in the supernatant of DPG3-stimulated WT macrophages (Fig. 4b), compared with P2X7$^{-/-}$ (Fig. 4c). In addition, pro-IL-1β levels in the supernatant were also higher for DPG3-stimulated WT cells (Fig. 4b), elucidating ELISA findings, since the ELISA kit used in this study does not distinguish between pro-IL-1β and the mature, secreted form of the cytokine. Interestingly, only the inactive form of the cytokine, pro-IL-1β, was found in the supernatant from P2X7$^{-/-}$ cells (Fig. 4c), confirming that P2X7-dependent signaling is crucial for IL-1β processing in *P. gingivalis*-infected cells. When caspase-1 activation was investigated in lysates, DPG3-stimulated WT cells possessed higher activated caspase-1 as compared to 381-stimulated cells. This was demonstrated by the decrease in pro-caspase and an increase in the active form (p20) from cells stimulated by the non-fimbriated *P. gingivalis* (Fig. 4d). With ATP addition, pro-caspase-1 was also decreased for DPG3-stimulated cells as compared to 381. This data further confirm the earlier observation that fimbriae reduce pro-IL-1β processing.

Pro-IL-1β mRNA and protein expression induced by *P. gingivalis* is TLR2- and MyD88-dependent but TLR4-independent

Since there is controversy regarding which Toll-like receptors (TLRs), TLR2 or TLR4 are stimulated by *P. gingivalis* infection [28–30], we wished to determine whether the first signal for pro-IL-1β production was TLR2- or TLR4-dependent and whether the absence of fimbriae was modulating IL-1β secretion due to its effect on the first signal. Thus, we used BMDMs derived from WT, TLR2$^{-/-}$, TLR4$^{-/-}$ and MyD88$^{-/-}$ mice to examine the effects of these TLRs or the adaptor protein, MyD88, on IL-1β mRNA and protein expression. qPCR analysis showed impaired IL-1β mRNA expression during *P. gingivalis* infection due to lack of TLR2 and MyD88 but not TLR4 (Fig. 5a). Consistent with a previous report [13], *P. gingivalis* stimulation of IL-1β mRNA was TLR2 dependent and the lack of fimbriae did not alter the TLR dependence. The importance of TLR2 and MyD88 for IL-1β production was confirmed at the protein level by ELISA in BMDM supernatants (Fig. 5b) and by Western blot of whole cell lysates and supernatants (Fig. 5c) with or without eATP treatment during *P. gingivalis* infection. We also observed a higher expression of IL-1β mRNA by 381-stimulated cells in the absence of TLR4 (Fig. 5a) which could be explained by a possible TLR2 compensatory upregulation leading to the observed IL-1β transcript.

DPG3-stimulated WT cells were more sensitive to P2X7-dependent eATP-induced early apoptosis

Given that eATP-P2X7 binding leads to pore formation and that there is a link between apoptosis and inflammasome activation [31], we next examined whether the differences in IL-1β secretion between 381- and DPG3-infected cells might be due to differences in cell death. For this, we quantified the percentage of apoptotic cells by Annexin V/Propidium Iodide (PI) staining (Fig. 6a) as well as cell lysis by lactate dehydrogenase (LDH) release from infected WT and P2X7$^{-/-}$ BMDMs (Fig. 6b and 6c). The results showed that, without eATP treatment, *P. gingivalis* infection did not induce apoptosis in WT cells (Fig. 6a upper panel), consistent with previous reports [32–35]. When eATP was added for 30 min to the 381-infected cells, *P. gingivalis* inhibited eATP-induced P2X7-dependent early apoptotic cells (percentage of annexin V+ PI− BMDMs), consistent with previous findings in gingival epithelial cells [35]. In contrast, DPG3-infected WT cells were more sensitive to eATP-induced, P2X7-dependent early apoptosis when compared to 381-infected cells, as seen in the percentage of annexin V+ PI− cells compared to medium-treated cells. The difference between 381- and DPG3-infected cells in the early stages of apoptosis was not observed in P2X7$^{-/-}$ cells (Fig. 6a, lower panel). In order to reinforce these data, we show the percentage of apoptotic cell death (Fig. 6b) as well as Western blot analysis for p-Bad and p-Stat3 expression (Fig. 6c and 6d). In Fig. 6c, we compare the phosphorylation of the protein Bad, which is a proapoptotic member of the Bcl-2 family. The expression of phosphorylated Bad was higher for DPG3-stimulated cells, mainly after eATP treatment. In addition, in Fig. 6d, we showed the higher activation of Stat3 signaling (p-Stat3 expression) in 381-stimulated cells. Since Stat-3 was demonstrated to confer resistance to apoptosis [36], this result supports the view that DPG3-stimulated cells are more sensitive to eATP-induced apoptosis. We also investigated the percentage of LDH release, which correlates with cell death, and found that there was very little LDH released from cells (less than 10%), with no significant differences between 381- and DPG3-infected BMDMs (Fig. 6e and 6f). When eATP was added to WT cells, there was a slight increase of LDH release for uninfected cells (almost 20% of LDH released) whereas no change was observed in *P. gingivalis*-infected cells (Fig. 6e).

P. gingivalis infection modulates P2X7 receptor distribution in a fimbriae-dependent manner

Given the importance of the P2X7 receptor for IL-1β secretion from *P. gingivalis*-infected cells, we next analyzed the cellular distribution of P2X7 receptor by an immunofluorescent study using confocal microscopy. BMDMs were infected at a MOI of 100 and analyzed 18h after infection followed by eATP stimulation. This study confirmed the presence of discrete P2X7 expression in the absence of *P. gingivalis* stimulation (Fig. 7a) which was enhanced by 381-stimulated cells (Fig. 7b). Notably, macrophages infected by the non-fimbriated *P.gingivalis* revealed a distinct pattern of P2X7 receptor with a markedly foci formation (Fig. 7c). The foci are particularly well visible in the enlarged image (Fig 1c; arrowheads) and clearly less prominent in cells stimulated by DPG3+Fim (Fig. 7d). Consistent with these results, the intracellular localization of the P2X7 receptor is well documented in other models [37–39]. The characteristic appearance as stained dots was reported to be distributed close to the membrane but also colocalized with the endoplasmatic reticulum [40].

Discussion

Inflammasome activation is necessary for IL-1β release and it comprises a two-step process involving a first signal triggered by the recognition of PAMPs and a second signal that is typically provided by DAMPs – also known as danger signals or alarmins – which are markers for cellular stress or damage, as may occur during infection [1]. Low IL-1β secretion during *P. gingivalis* infection may be explained by the fact that *P. gingivalis* infection can induce IL-1β at the transcriptional level (first signal) but is not a potent inducer for post-translational conversion to the IL-1β mature form (second signal) in primary BMDMs. The ability of *P. gingivalis* to stimulate the first but not the second signal may be a rare trait of periodontopathogens [17]. In addition, it is known that subgingival biofilms down-regulate NLRP3 and IL-1β gene expression in gingival fibroblasts *in vitro*, with *P. gingivalis* being a critical component of the biofilms [41]. The present literature supports the notion that, as part of the polymicrobial community, *P. gingivalis* can disrupt host-microbial homeostasis by dampening the pathogen-sensing capacity of the host cells via inflammasomes [42].

This is the first study to report that *P. gingivalis* actively altered IL-1β secretion by primary macrophages by means of its fimbriae and that this occurred through a P2X7 receptor-dependent manner. It has been reported previously [17] that *P. gingivalis* can inhibit *Fusobacterium nucleatum*-mediated IL-1β secretion without reducing *F. nucleatum*-induced IL-1β transcript levels, suggesting a suppressive effect at the post-translational level. *P. gingivalis* fimbriae were also reported to elicit differential production of cytokines from the IL-1 family (IL-1β/IL-18) from human monocytes/macrophages [43–45]. Furthermore, *P. gingivalis* can suppress the secretion of IL-18, another cytokine that is known to be processed by the inflammasome, without affecting the levels of its transcripts [17]. These results suggest that inflammasome inhibition by *P. gingivalis* occurred at the second signal level. Our current study demonstrates that *P. gingivalis* fimbriae are able to inhibit IL-1β at the second signal level by interfering with ATP signaling through the purinergic receptor, P2X7. A recent work [46] reported that *P. gingivalis* activates ATP release and that the inhibition of K^+ efflux by increasing extracellular K^+ concentration blocked caspase-1 activation, IL-1β secretion, and pyroptic cell death induced by this pathogen. Here, we showed that this mechanism of IL-1β secretion by *P. gingivalis* is not only dependent of K^+ efflux but it also involves the participation of $iPLA_2$ which is related to fusion of secretory lysosomes with the plasma membrane in the non-classical secretory events induced by eATP stimulation [25].

P2X7 receptor signaling has been shown to be important in innate immune responses, especially for control of infection by intracellular pathogens. It was reported that P2X7 ligation limits infection of macrophages or epithelial cells by *Chlamydia trachomatis* or of the murine strain, *Chlamydia muridarum*. ATP-induced chlamydial killing is impaired in peritoneal macrophages from P2X7-deficient mice, thereby, supporting a role for P2X7 in this process [47,48]. Although inflammasome activation in response to infection by intracellular pathogens has been well investigated, only a few studies have addressed the role of P2X7 in *P. gingivalis* infection. It has been demonstrated that *P. gingivalis* can inhibit ATP-induced, P2X7-dependent gingival epithelial cell apoptosis [35] and inhibit ATP-induced reactive oxygen species generation via P2X7 receptor/NADPH-oxidase signaling [49], thus contributing to the survival of the bacterium in the host. The present findings corroborate that *P. gingivalis* infection impairs ATP-induced apoptosis, adding that the inhibition occurs by means of its fimbriae and through the P2X7 receptor.

Many studies on *P. gingivalis* subversion mechanisms have been carried out, showing that this microorganism can exploit many mechanisms to use host cells in its favor for immune manipulation and consequently to allow its persistence in the host [50]. By means of its fimbriae, *P. gingivalis* can bind CXC-chemokine receptor 4 and induce crosstalk with TLR2, inhibiting the MyD88-dependent antimicrobial pathway [51]. A recent study showed that during early stages of infection, IL-10 production following *P. gingivalis* stimulation is fimbriae-dependent, which can suppress the immune response by inhibiting robust inflammatory cytokines [52]. In the present study we showed that *P. gingivalis* stimulation of IL-1β mRNA and protein depended strongly on the activation of TLR2 and MyD88, and the lack of fimbriae did not affect this outcome, corroborating previous work [13]. Moreover, we observed higher levels of IL-1β mRNA in TLR4−/− cells. Previous studies have shown that macrophages from TLR4-deficient C3H/HeJ mice upregulated expression of TLR2 [53] and that cytokines such as IL-1β were enhanced in TLR2+/4− mice exposed to *Mycoplasma arthritidis*, an inflammatory murine pathogen [54].

We have shown that the absence of *P. gingivalis* fimbriae affected the kinetics of pro-IL-1β expression at the transcriptional level. In the presence of eATP as a second signal, less pro-IL-1β was found in the cell lysate and more was secreted to the supernatant. Here, we propose that IL-1β processing was increased in the absence of fimbriae, presumably reflecting higher sensibility of macrophages to the danger signal eATP. The finding that non-fimbriated *P. gingivalis* did not inhibit apoptosis induced by this potent danger signal further underscores the pathogenic role of fimbriae in *P. gingivalis* infection. Although there is a precedent that *P. gingivalis* inhibits apoptosis induced by eATP ligation to P2X7 receptors expressed in gingival epithelial cells [35], our study is the first to implicate fimbriae as the bacterial factor that limits eATP-induced apoptosis of macrophages via the P2X7 signaling pathway. We demonstrated here that non-fimbriated *P. gingivalis* did not induce p-STAT3 expression compared with 381-stimulated cells. Indeed, STAT3, a transcription factor involved in IL-6 signaling, was demonstrated to also have anti-apoptotic activity [36]. On the other hand, when we investigated the expression of p-Bad, which is a proapoptotic member of the Bcl-2 family, we found a higher level of expression in DPG3-stimulated cells, further implicating fimbriae as a bacterial virulence factor that limits eATP-induced apoptosis of macrophages. Furthermore, when we investigated the P2X7 receptor distribution by immunofluorescence and confocal microscopy it was clearly visible that the non-fimbriated *P.gingivalis* induced a distinct pattern of P2X7 receptor arrangement with stained points concentrated in the cells. This concentration of P2X7 receptor as stained points was already reported previously by another study [40] and although speculative it could be one of the possibilities of a more pronounced signaling via P2X7 receptor leading to a higher IL-1β secretion observed by DPG3-stimulated cells.

P. gingivalis has already been reported to inhibit P2X7-dependent signaling using secreted nucleoside diphosphate kinase (NDK), which consumes eATP and prevents apoptosis [35]. Furthermore, this was shown to be through mitochondrial ROS generated through P2X7 [49]. However, we believe that the mechanism of inhibition is different for fimbriae, which are not known to degrade eATP. Here, we hypothesize that the lack of fimbriae may induce a higher level of cleavage of pro-IL-1β, resulting in a larger quantity of secreted mature IL-1β. We demonstrated here that non-fimbriated *P. gingivalis* induced higher caspase-1 processing compared to 381-stimulated cells, as demonstrated by the decrease in pro-caspase and increase of the active form (p20). Intriguingly, more pro-IL-1β was also secreted by macrophage in a P2X7-dependent manner. In addition, it is worthwhile mentioning that these findings were independent of bacteria viability, since the same effect was elicited by heat-killed *P. gingivalis* (data not shown). Moreover, the repression of IL-1β secretion by *P. gingivalis* fimbriae did not hinder the secretion of other cytokines which are usually secreted by a canonical pathway such as TNF-α, IL-10, CXCL-1 and IL-6, and do not directly depend on the inflammasome. Also, their production was independent of eATP stimulation through the P2X7 receptor.

In conclusion, this study provided new experimental evidence linking the immune subversion activity of *P. gingivalis* to the ability of fimbriae to limit eATP-induced macrophage secretion of IL-1β via P2X7 activation. A better understanding of the role of the axis eATP-P2X7 in IL-1β secretion and the mechanisms that can control this pathway will further contribute to the advance of our knowledge on inflammatory conditions.

Supplementary Material

Refer to Web version on PubMed Central for supplementary material.

Acknowledgments

This work was supported by funds from the Conselho Nacional de Desenvolvimento Cientifico e Tecnológico do Brasil (CNPq), Coordenação de Aperfeiçoamento de Pessoal de Nível Superior (CAPES), the Programa de Núcleos de Excelência (PRONEX), Fundação de Amparo à Pesquisa do Estado do Rio de Janeiro (FAPERJ) and the Instituto Nacional de Ciência e Tecnologia para Pesquisa Translacional em Saúde e Ambiente na Região Amazônica (INPeTAm/UFRJ). This study was approved and partially funded by Ciências sem Fronteiras Federal Government Program with post-doc scholarship to ACM. This work was also partially supported by National Institutes of Health grants R01DE019444 and NIDCR/DE 09761 to DMO and JP, respectively.

Abbreviations used in this article

P2X7	P2X purinergic receptor 7
WT	wild-type
Fim	fimbriae
BMDM	bone marrow derived macrophage
Nlrp3	NLR pyrin domain-containing 3

dLN	draining lymph (node) cell
BEL	Bromoenol Lactone

References

1. Said-Sadier N, Ojcius DM. Alarmins, inflammasomes and immunity. Biomed J. 2012; 35:437–449. [PubMed: 23442356]
2. Fantuzzi G, Dinarello CA. Interleukin-18 and interleukin-1 beta: Two cytokine substrates for ice (caspase-1). J Clin Immunol. 1999; 19:1–11. [PubMed: 10080100]
3. Abdul-Sater AA, Said-Sadier N, Ojcius DM, Yilmaz O, Kelly KA. Inflammasomes bridge signaling between pathogen identification and the immune response. Drugs Today (Barc). 2009; 45(Suppl B): 105–112. [PubMed: 20011701]
4. Netea MG, Nold-Petry CA, Nold MF, Joosten LA, Opitz B, van der Meer JH, van de Veerdonk FL, Ferwerda G, Heinhuis B, Devesa I, Funk CJ, Mason RJ, Kullberg BJ, Rubartelli A, van der Meer JW, Dinarello CA. Differential requirement for the activation of the inflammasome for processing and release of IL-1beta in monocytes and macrophages. Blood. 2009; 113:2324–2335. [PubMed: 19104081]
5. Eder C. Mechanisms of interleukin-1beta release. Immunobiology. 2009; 214:543–553. [PubMed: 19250700]
6. Lamkanfi M, Dixit VM. Inflammasomes: Guardians of cytosolic sanctity. Immunol Rev. 2009; 227:95–105. [PubMed: 19120479]
7. Martinon F, Burns K, Tschopp J. The inflammasome: A molecular platform triggering activation of inflammatory caspases and processing of pro-IL1-beta. Mol Cell. 2002; 10:417–426. [PubMed: 12191486]
8. Rathinam VA, Vanaja SK, Fitzgerald KA. Regulation of inflammasome signaling. Nat Immunol. 2012; 13:333–332. [PubMed: 22430786]
9. Taxman DJ, Huang MT, Ting JP. Inflammasome inhibition as a pathogenic stealth mechanism. Cell Host Microbe. 2010; 8:7–11. [PubMed: 20638636]
10. Darveau RP, Hajishengallis G, Curtis MA. *Porphyromonas gingivalis* as a potential community activist for disease. J Dent Res. 2012; 91:816–820. [PubMed: 22772362]
11. Hajishengallis G, Wang M, Liang S, Triantafilou M, Triantafilou K. Pathogen induction of cxcr4/tlr2 cross-talk impairs host defense function. Proc Natl Acad Sci U S A. 2008; 105:13532–13537. [PubMed: 18765807]
12. Guo Y, Nguyen KA, Potempa J. Dichotomy of gingipains action as virulence factors: From cleaving substrates with the precision of a surgeon’s knife to a meat chopper-like brutal degradation of proteins. Periodontol 2000. 2010; 54:15–44. [PubMed: 20712631]
13. Papadopoulos G, Weinberg EO, Massari P, Gibson FC 3rd, Wetzler LM, Morgan EF, Genco CA. Macrophage-specific tlr2 signaling mediates pathogen-induced tnf-dependent inflammatory oral bone loss. J Immunol. 2013; 190:1148–1157. [PubMed: 23264656]
14. Yilmaz O, Sater AA, Yao L, Koutouzis T, Pettengill M, Ojcius DM. Atp-dependent activation of an inflammasome in primary gingival epithelial cells infected by *Porphyromonas gingivalis*. Cell Microbiol. 2010; 12:188–198. [PubMed: 19811501]
15. Persechini PM, Bisaggio RC, Alves-Neto JL, Coutinho-Silva R. Extracellular atp in the lymphohematopoietic system: P2z purinoceptors off membrane permeabilization. Braz J Med Biol Res. 1998; 31:25–34. [PubMed: 9686176]
16. Coutinho-Silva R, Ojcius DM. Role of extracellular nucleotides in the immune response against intracellular bacteria and protozoan parasites. Microbes Infect. 2012; 14:1271–1277. [PubMed: 22634346]
17. Taxman DJ, Swanson KV, Broglie PM, Wen H, Holley-Guthrie E, Huang MT, Callaway JB, Eitas TK, Duncan JA, Ting JP. *Porphyromonas gingivalis* mediates inflammasome repression in polymicrobial cultures through a novel mechanism involving reduced endocytosis. J Biol Chem. 2012; 287:32791–32799. [PubMed: 22843689]

18. Davis BK, Wen H, Ting JP. The inflammasome nlrs in immunity, inflammation, and associated diseases. Annu Rev Immunol. 2011; 29:707–735. [PubMed: 21219188]
19. Oliveira AC, de Alencar BC, Tzelepis F, Klezewsky W, da Silva RN, Neves FS, Cavalcanti GS, Boscardin S, Nunes MP, Santiago MF, Nobrega A, Rodrigues MM, Bellio M. Impaired innate immunity in tlr4(−/−) mice but preserved cd8+ t cell responses against trypanosoma cruzi in tlr4-, tlr2-, tlr9- or myd88-deficient mice. PLoS Pathog. 2010; 6:e1000870. [PubMed: 20442858]
20. Rapala-Kozik M, Bras G, Chruscicka B, Karkowska-Kuleta J, Sroka A, Herwald H, Nguyen KA, Eick S, Potempa J, Kozik A. Adsorption of components of the plasma kinin-forming system on the surface of *Porphyromonas gingivalis* involves gingipains as the major docking platforms. Infect Immun. 2011; 79:797–805. [PubMed: 21098107]
21. Monteiro AC, Scovino A, Raposo S, Gaze VM, Cruz C, Svensjo E, Narciso MS, Colombo AP, Pesquero JB, Feres-Filho E, Nguyen KA, Sroka A, Potempa J, Scharfstein J. Kinin danger signals proteolytically released by gingipain induce fimbriae-specific ifn-gamma- and il-17-producing t cells in mice infected intramucosally with porphyromonas gingivalis. J Immunol. 2009; 183:3700–3711. [PubMed: 19687097]
22. Hamada N, Sojar HT, Cho MI, Genco RJ. Isolation and characterization of a minor fimbria from *Porphyromonas gingivalis*. Infect Immun. 1996; 64:4788–4794. [PubMed: 8890240]
23. Marim FM, Silveira TN, Lima DS Jr, Zamboni DS. A method for generation of bone marrow-derived macrophages from cryopreserved mouse bone marrow cells. PLoS One. 2010; 5:e15263. [PubMed: 21179419]
24. Coutinho-Silva R, Perfettini JL, Persechini PM, Dautry-Varsat A, Ojcius DM. Modulation of p2z/p2x(7) receptor activity in macrophages infected with *Chlamydia psittaci*. Am J Physiol Cell Physiol. 2001; 280:C81–89. [PubMed: 11121379]
25. Andrei C, Margiocco P, Poggi A, Lotti LV, Torrisi MR, Rubartelli A. Phospholipases c and a2 control lysosome-mediated IL-1 beta secretion: Implications for inflammatory processes. Proc Natl Acad Sci U S A. 2004; 101:9745–9750. [PubMed: 15192144]
26. Di Virgilio F, Chiozzi P, Ferrari D, Falzoni S, Sanz JM, Morelli A, Torboli M, Bolognesi G, Baricordi OR. Nucleotide receptors: An emerging family of regulatory molecules in blood cells. Blood. 2001; 97:587–600. [PubMed: 11157473]
27. Franchi L, Chen G, Marina-Garcia N, Abe A, Qu Y, Bao S, Shayman JA, Turk J, Dubyak GR, Nunez G. Calcium-independent phospholipase a2 beta is dispensable in inflammasome activation and its inhibition by bromoenol lactone. J Innate Immun. 2009; 1:607–617. [PubMed: 20160900]
28. Coats SR, Jones JW, Do CT, Braham PH, Bainbridge BW, To TT, Goodlett DR, Ernst RK, Darveau RP. Human toll-like receptor 4 responses to *P. gingivalis* are regulated by lipid a 1- and 4′-phosphatase activities. Cell Microbiol. 2009; 11:1587–1599. [PubMed: 19552698]
29. Curtis MA, Percival RS, Devine D, Darveau RP, Coats SR, Rangarajan M, Tarelli E, Marsh PD. Temperature-dependent modulation of *Porphyromonas gingivalis* lipid a structure and interaction with the innate host defenses. Infect Immun. 2011; 79:1187–1193. [PubMed: 21220483]
30. Jain S, Coats SR, Chang AM, Darveau RP. A novel class of lipoprotein lipase-sensitive molecules mediates toll-like receptor 2 activation by *Porphyromonas gingivalis*. Infect Immun. 2013; 81:1277–1286. [PubMed: 23381996]
31. Shimada K, Crother TR, Karlin J, Dagvadorj J, Chiba N, Chen S, Ramanujan VK, Wolf AJ, Vergnes L, Ojcius DM, Rentsendorj A, Vargas M, Guerrero C, Wang Y, Fitzgerald KA, Underhill DM, Town T, Arditi M. Oxidized mitochondrial DNA activates the nlrp3 inflammasome during apoptosis. Immunity. 2012; 36:401–414. [PubMed: 22342844]
32. Mao S, Park Y, Hasegawa Y, Tribble GD, James CE, Handfield M, Stavropoulos MF, Yilmaz O, Lamont RJ. Intrinsic apoptotic pathways of gingival epithelial cells modulated by *Porphyromonas gingivalis*. Cell Microbiol. 2007; 9:1997–2007. [PubMed: 17419719]
33. Yilmaz O, Jungas T, Verbeke P, Ojcius DM. Activation of the phosphatidylinositol 3-kinase/akt pathway contributes to survival of primary epithelial cells infected with the periodontal pathogen *Porphyromonas gingivalis*. Infect Immun. 2004; 72:3743–3751. [PubMed: 15213114]
34. Yilmaz O, Verbeke P, Lamont RJ, Ojcius DM. Intercellular spreading of *Porphyromonas gingivalis* infection in primary gingival epithelial cells. Infect Immun. 2006; 74:703–710. [PubMed: 16369027]

35. Yilmaz O, Yao L, Maeda K, Rose TM, Lewis EL, Duman M, Lamont RJ, Ojcius DM. Atp scavenging by the intracellular pathogen *Porphyromonas gingivalis* inhibits p2x7-mediated host-cell apoptosis. Cell Microbiol. 2008; 10:863–875. [PubMed: 18005240]
36. Catlett-Falcone R, Landowski TH, Oshiro MM, Turkson J, Levitzki A, Savino R, Ciliberto G, Moscinski L, Fernandez-Luna JL, Nunez G, Dalton WS, Jove R. Constitutive activation of stat3 signaling confers resistance to apoptosis in human u266 myeloma cells. Immunity. 1999; 10:105–115. [PubMed: 10023775]
37. Atkinson L, Milligan CJ, Buckley NJ, Deuchars J. An atp-gated ion channel at the cell nucleus. Nature. 2002; 420:42. [PubMed: 12422208]
38. Bardini M, Lee HY, Burnstock G. Distribution of p2x receptor subtypes in the rat female reproductive tract at late pro-oestrus/early oestrus. Cell Tissue Res. 2000; 299:105–113. [PubMed: 10654074]
39. Lee HY, Bardini M, Burnstock G. Distribution of p2x receptors in the urinary bladder and the ureter of the rat. J Urol. 2000; 163:2002–2007. [PubMed: 10799247]
40. Antonio LS, Costa RR, Gomes MD, Varanda WA. Mouse leydig cells express multiple p2x receptor subunits. Purinergic Signal. 2009; 5:277–287. [PubMed: 19020992]
41. Belibasakis GN, Guggenheim B, Bostanci N. Down-regulation of nlrp3 inflammasome in gingival fibroblasts by subgingival biofilms: Involvement of *Porphyromonas gingivalis*. Innate Immun. 2013; 19:3–9. [PubMed: 22522430]
42. Bostanci N, Emingil G, Saygan B, Turkoglu O, Atilla G, Curtis MA, Belibasakis GN. Expression and regulation of the nalp3 inflammasome complex in periodontal diseases. Clin Exp Immunol. 2009; 157:415–422. [PubMed: 19664151]
43. Hajishengallis G, Martin M, Schifferle RE, Genco RJ. Counteracting interactions between lipopolysaccharide molecules with differential activation of toll-like receptors. Infect Immun. 2002; 70:6658–6664. [PubMed: 12438339]
44. Hamedi M, Belibasakis GN, Cruchley AT, Rangarajan M, Curtis MA, Bostanci N. *Porphyromonas gingivalis* culture supernatants differentially regulate interleukin-1beta and interleukin-18 in human monocytic cells. Cytokine. 2009; 45:99–104. [PubMed: 19091595]
45. Sugano N, Ikeda K, Oshikawa M, Sawamoto Y, Tanaka H, Ito K. Differential cytokine induction by two types of *Porphyromonas gingivalis*. Oral Microbiol Immunol. 2004; 19:121–123. [PubMed: 14871353]
46. Park E, Na HS, Song YR, Shin SY, Kim YM, Chung J. Activation of nlrp3 and aim2 inflammasomes by *Porphyromonas gingivalis* infection. Infect Immun. 2014; 82:112–123. [PubMed: 24126516]
47. Coutinho-Silva R, Stahl L, Raymond MN, Jungas T, Verbeke P, Burnstock G, Darville T, Ojcius DM. Inhibition of chlamydial infectious activity due to p2x7r-dependent phospholipase d activation. Immunity. 2003; 19:403–412. [PubMed: 14499115]
48. Darville T, Welter-Stahl L, Cruz C, Sater AA, Andrews CW Jr, Ojcius DM. Effect of the purinergic receptor p2x7 on *Chlamydia* infection in cervical epithelial cells and vaginally infected mice. J Immunol. 2007; 179:3707–3714. [PubMed: 17785807]
49. Choi CH, Spooner R, Deguzman J, Koutouzis T, Ojcius DM, Yilmaz O. *Porphyromonas gingivalis*-nucleoside-diphosphate-kinase inhibits atp-induced reactive-oxygen-species via p2x7 receptor/nadph-oxidase signalling and contributes to persistence. Cell Microbiol. 2013; 15:961–976. [PubMed: 23241000]
50. Hajishengallis G, Darveau RP, Curtis MA. The keystone-pathogen hypothesis. Nat Rev Microbiol. 2012; 10:717–725. [PubMed: 22941505]
51. Hajishengallis G, McIntosh ML, Nishiyama SI, Yoshimura F. Mechanism and implications of cxcr4-mediated integrin activation by *Porphyromonas gingivalis*. Mol Oral Microbiol. 2012
52. Gaddis DE, Maynard CL, Weaver CT, Michalek SM, Katz J. Role of tlr2-dependent il-10 production in the inhibition of the initial ifn-gamma t cell response to *Porphyromonas gingivalis*. J Leukoc Biol. 2013; 93:21–31. [PubMed: 23077245]
53. Mu HH, Pennock ND, Humphreys J, Kirschning CJ, Cole BC. Engagement of toll-like receptors by mycoplasmal superantigen: Downregulation of tlr2 by mam/tlr4 interaction. Cell Microbiol. 2005; 7:789–797. [PubMed: 15888082]

54. Mu HH, Hasebe A, Van Schelt A, Cole BC. Novel interactions of a microbial superantigen with tlr2 and tlr4 differentially regulate il-17 and th17-associated cytokines. Cell Microbiol. 2011; 13:374–387. [PubMed: 20946245]

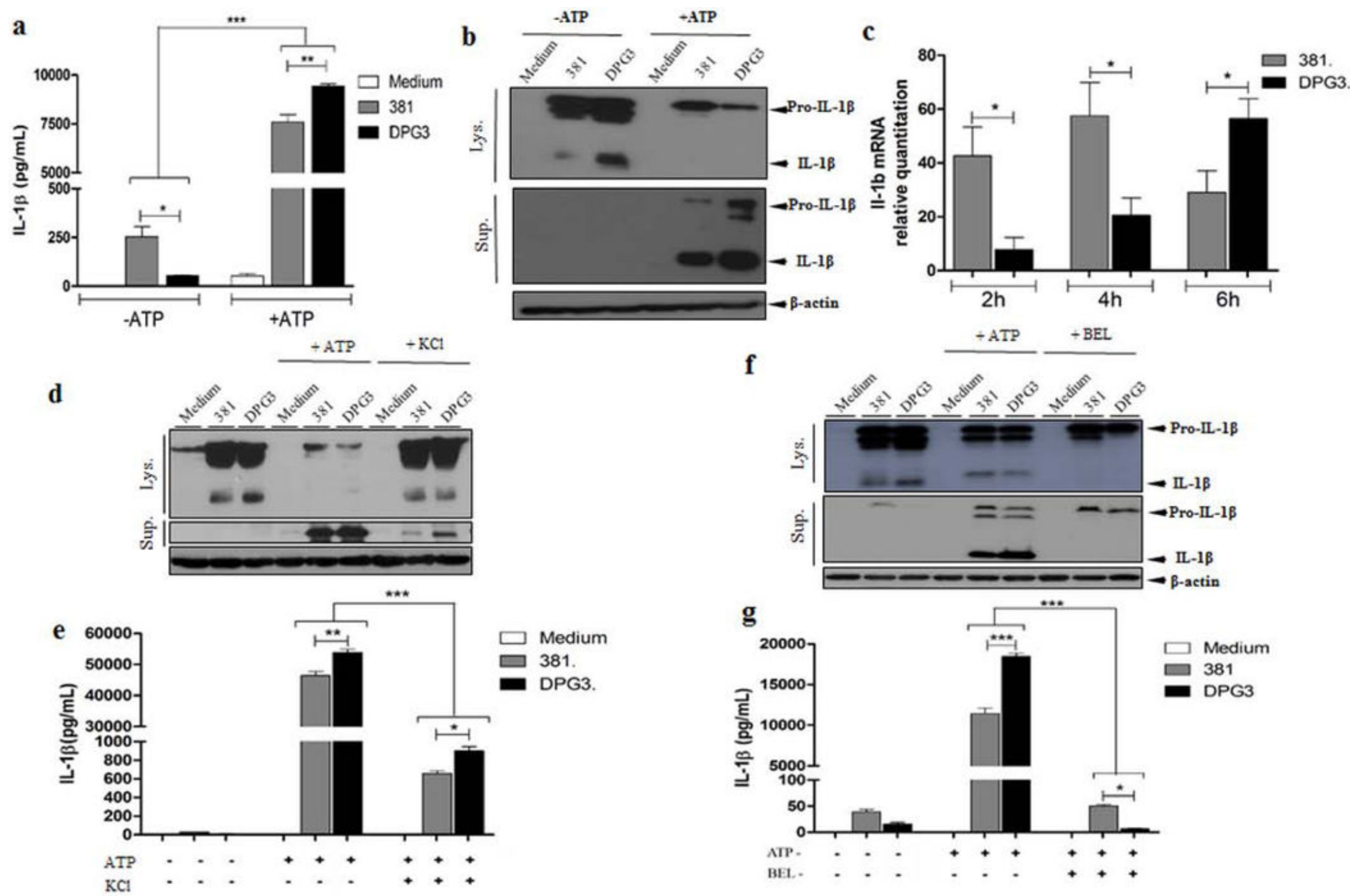

Figure 1. *P. gingivalis* impairs IL-1β secretion by means of its fimbriae only after eATP stimulation and this is dependent of K^+ efflux and phospholipase activity

(a) IL-1β secretion was analyzed by ELISA in BMDMs from C57BL/6 mice in response to eATP stimulation. Culture supernatants were collected after 18 h of infection with *P. gingivalis* strains 381 or DPG3 (MOI of 100) and subsequent incubation with or without 5 mM eATP for 30 min. **(b)** Pro-IL-1β and mature IL-1β detected in cell lysates (upper panel) and cell supernatants (lower panel) after 6 h of *P. gingivalis* infection or *P. gingivalis* infection plus eATP as described in Methods. β-actin was used as a loading control. **(c)** BMDMs were infected with 381 or DPG3 strain of *P. gingivalis* for the indicated time. Total RNA from each group was extracted, reverse transcribed, and quantified by quantitative PCR. After *P.gingivalis* infection for 5h, BMDMs were treated with **(d, e)** KCl (50mM) or **(f, g)** BEL (40μM) for an additional 1h and then incubated with or without 5 mM eATP for 30 min to measure IL-1β by Western blot and ELISA. Data are shown as mean ± SD and are representative of three independent experiments. Asterisk indicates a significant difference compared with indicated treatment group. *p <0.05, **p<0.01, ***p<0.001.

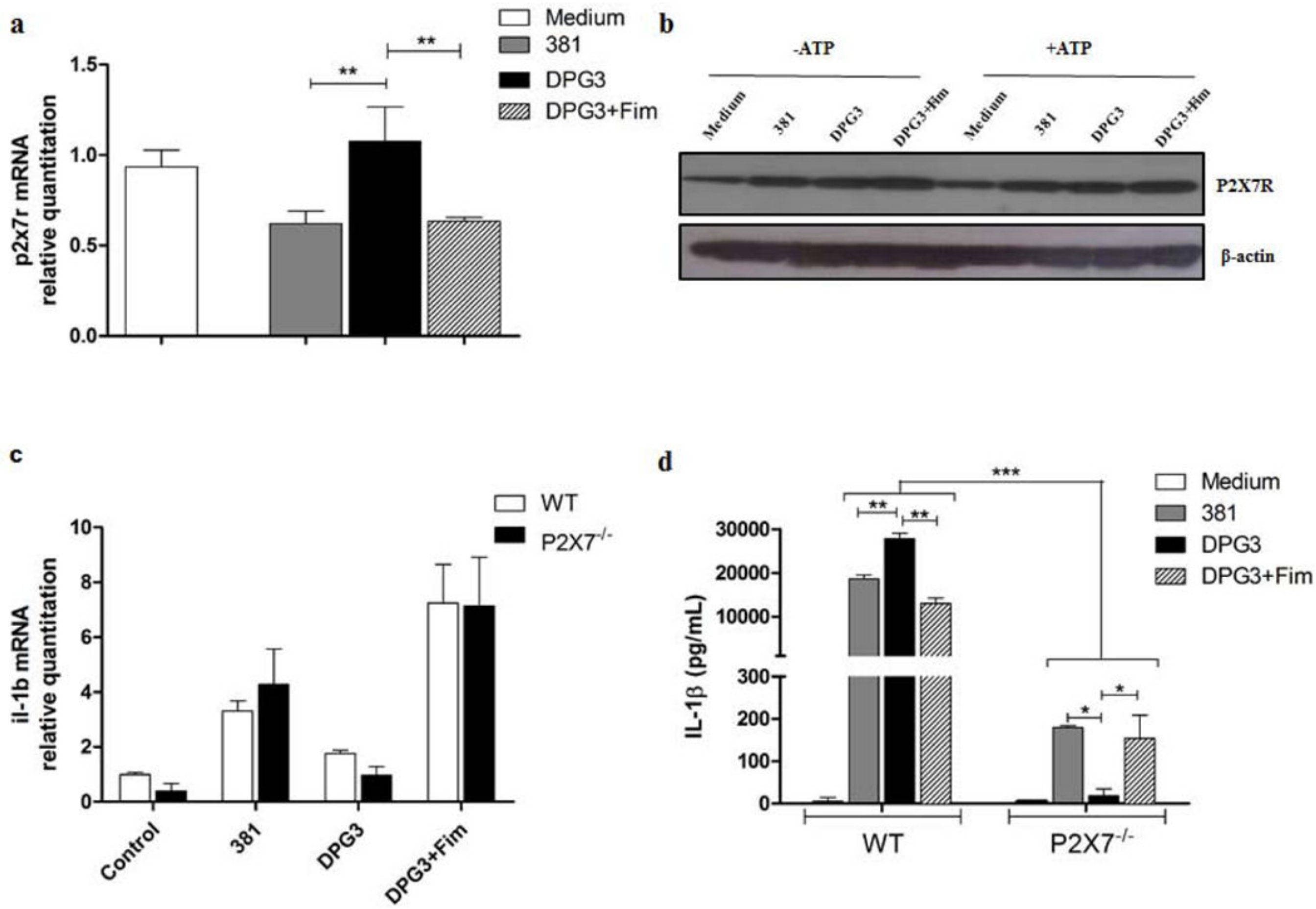

Figure 2. P2X7 receptor is required for fimbriae-impaired IL-1β secretion in *P. gingivalis* stimulated cells

(a) *P2x7* mRNA expression in BMDMs stimulated by *P. gingivalis* strains 381 or DPG3, or DPG3 complemented with recombinant Fim (DFi), at an MOI of 100 for 2 h. Total RNA from each group was extracted, reverse transcribed, and quantified by qPCR. **(b)** P2X7 expression in whole cell extracts infected with *P. gingivalis* for 18 h followed or not by 5 mM eATP stimulation for 30 min. **(c)** IL-1β mRNA expression comparing WT and P2X7$^{-/-}$ BMDMs stimulated with 381 or DPG3, or DPG3 with Fim. **(d)** IL-1β secretion analyzed by ELISA in BMDM supernatant from WT and P2X7$^{-/-}$ mice in response to eATP stimulation. Data are shown as mean ± SD and are representative of two independent experiments. Asterisk indicates a significant difference compared with indicated treatment group. *p <0.05, **p<0.01, ***p<0.001.

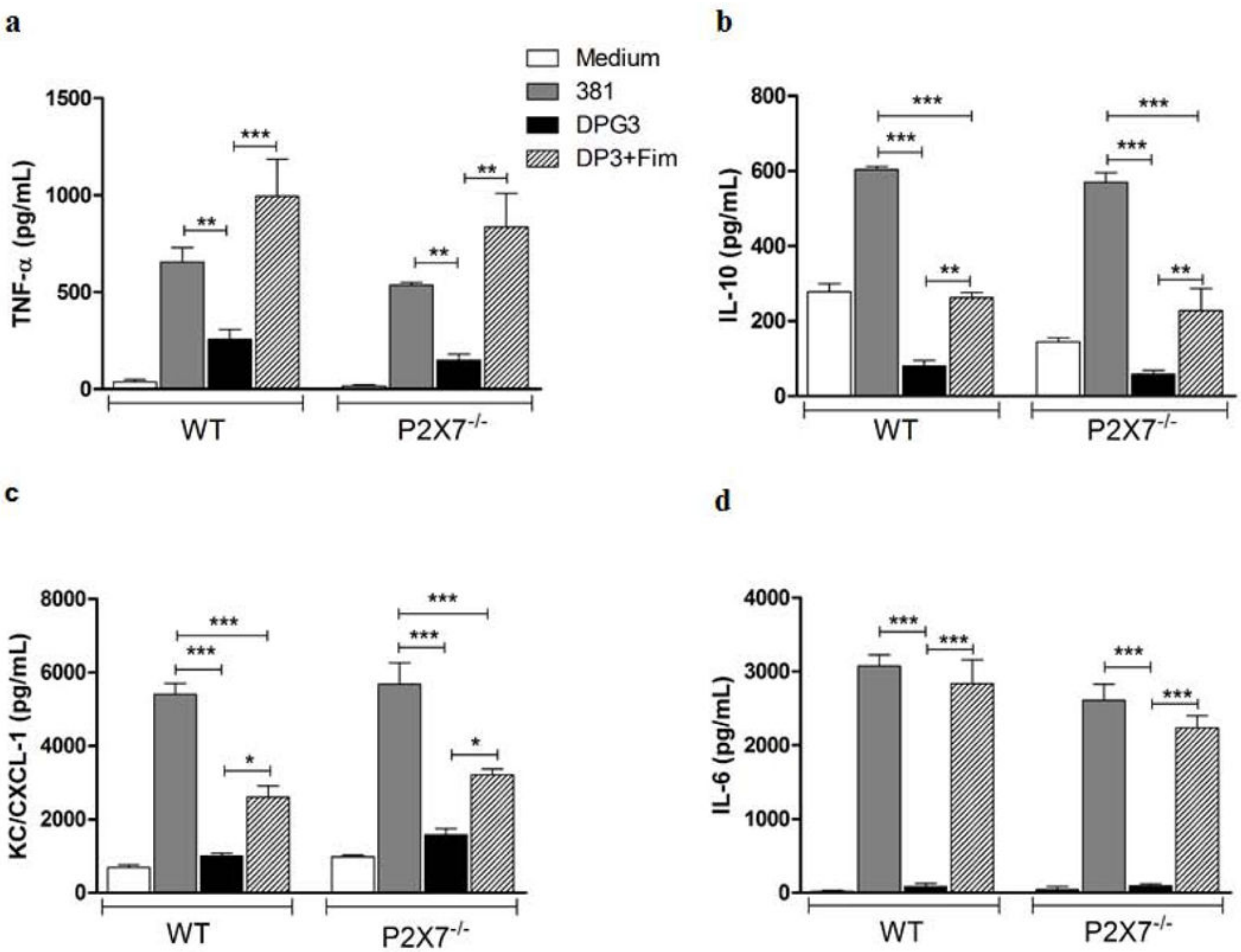

Figure 3. P2X7 receptor is dispensable for *P. gingivalis*-induced TNF-α, IL-10, CXCL1 and IL-6 secretion

TNF-α **(a)**, IL-10 **(b)**, CXCL1 **(c)** and IL-6 **(d)** secretion were analyzed by ELISA in BMDM supernatants from WT and P2X7$^{-/-}$ mice in response to eATP stimulation. Culture supernatants were collected after 18 h of infection with *P. gingivalis* strains 381 or DPG3, or DPG3 and Fim (MOI of 100) followed by 5 mM eATP for 30 min. Data are shown as mean ± SD and are representative of three independent experiments. Asterisk indicates a significant difference compared with indicated treatment group. $^*p<0.05$, $^{**}p<0.01$, $^{***}p<0.001$.

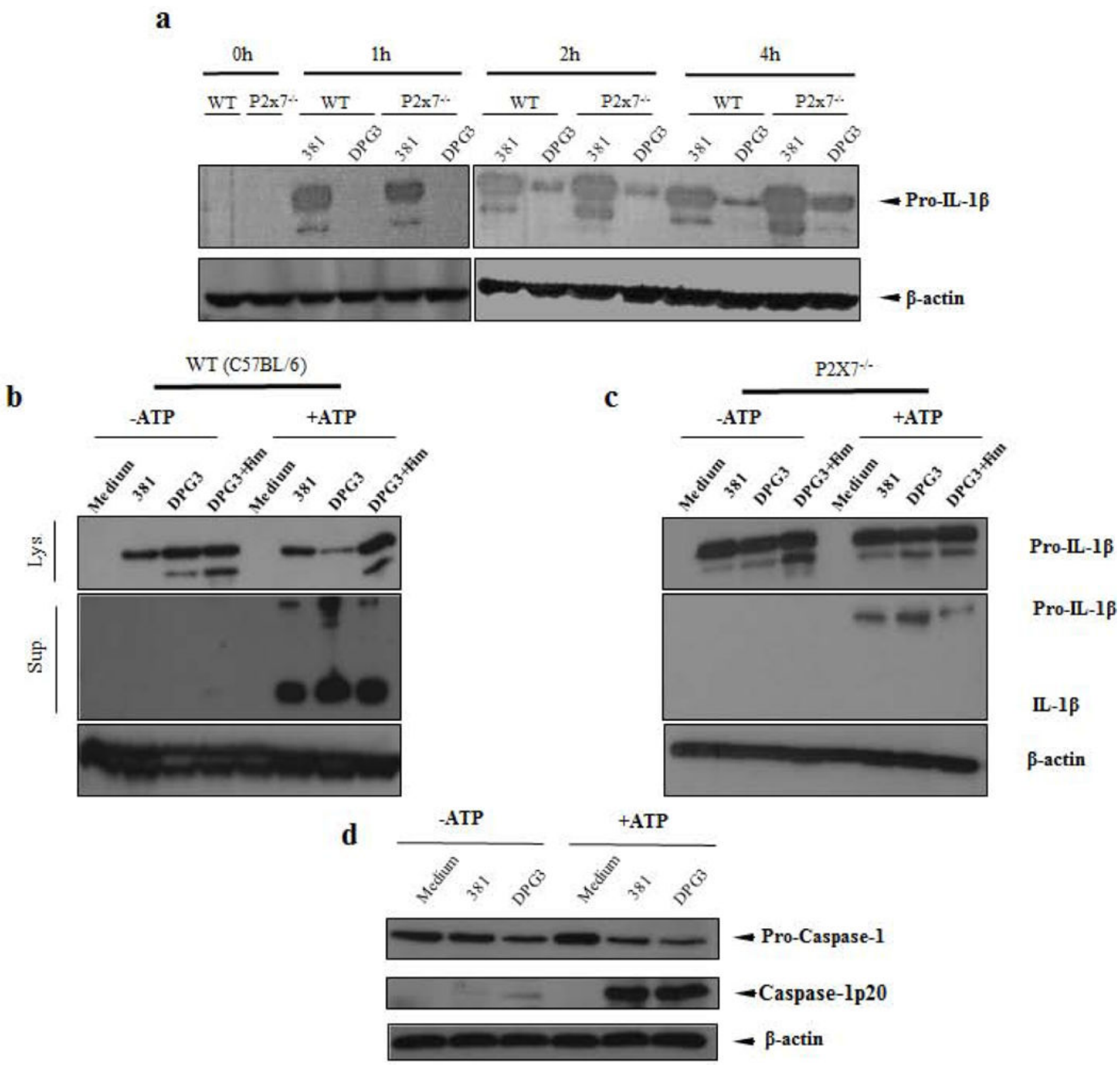

Figure 4. Pro-IL-1β processing induced by non-fimbriated *P. gingivalis* is higher than wild-type *P. gingivalis*, and mediated by P2X7 receptor ligation

(a) Kinetics of pro-IL-1β detected in whole cell lysates after 1 h, 2 h and 4 h of *P. gingivalis* infection of BMDMs from WT and P2X7$^{-/-}$ mice. Pro-IL-1β detected in whole cell lysates (lys.) and the mature IL-1β present in supernatants (sup.) after 18 h of *P. gingivalis* infection of BMDMs from **(b)** WT and **(c)** P2X7$^{-/-}$ mice with or without subsequent 5 mM eATP stimulation for 30 min as a second signal. **(d)** Whole cell lysates were analysed for caspase-1 activation comparing 381 and DPG3-stimulated WT cells with or without ATP addition for 30 min. Data are representative of two independent experiments for all situations.

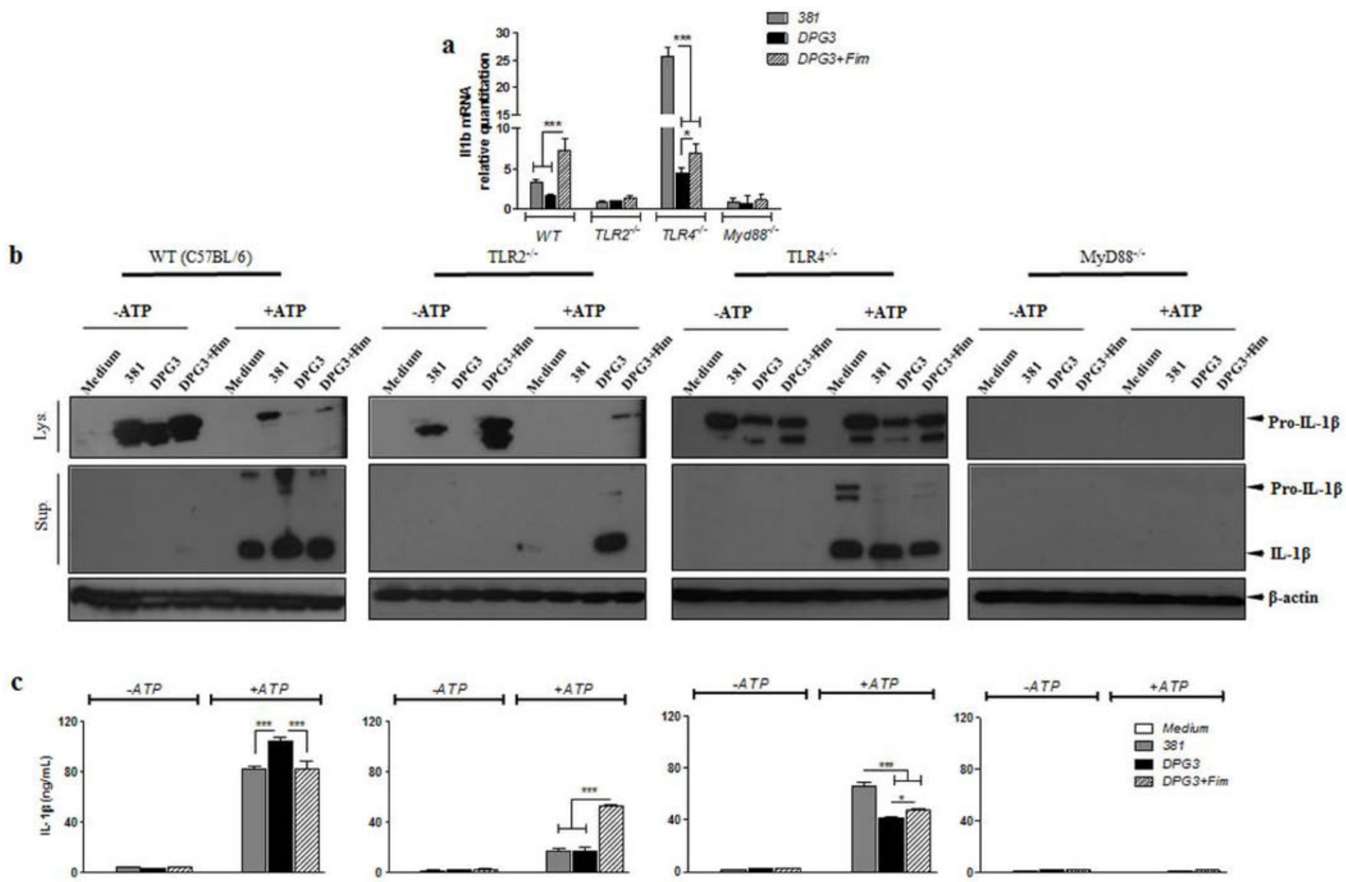

Figure 5. IL-1β mRNA and protein expression induced by *P. gingivalis* is TLR2 and MyD88-dependent but TLR4-independent

(a) IL-1β mRNA expression comparing WT to *tlr2*$^{-/-}$, *tlr4*$^{-/-}$ and *myd88*$^{-/-}$ BMDMs infected with *P. gingivalis* 381 or DPG3, or DPG3 and Fim (MOI of 100). Total RNA from each group was extracted, reverse transcribed, and quantified by qPCR. Data are shown as mean ± SD and are representative of two independent experiments. **(b)** IL-1β secretion was analyzed by ELISA comparing WT to *tlr2−/−*, *tlr4−/−* and *myd88−/−* cells in response to eATP stimulation. Culture supernatants were collected after 18 h of infection with *P. gingivalis* strains 381 or DPG3, or DPG3 infection and Fim stimulation (MOI of 100) followed or not by 5 mM eATP incubation for 30 min. **(c)** Pro-IL-1β and mature IL-1β detected in cell lysates (upper panel) and cell supernatants (lower panel) after 6 h of *P. gingivalis* infection or *P. gingivalis* infection plus eATP stimulation as described in Methods. β-actin was used as a loading control. Asterisk indicates a significant difference compared with indicated treatment group. *p <0.05, **p<0.01, ***p<0.001.

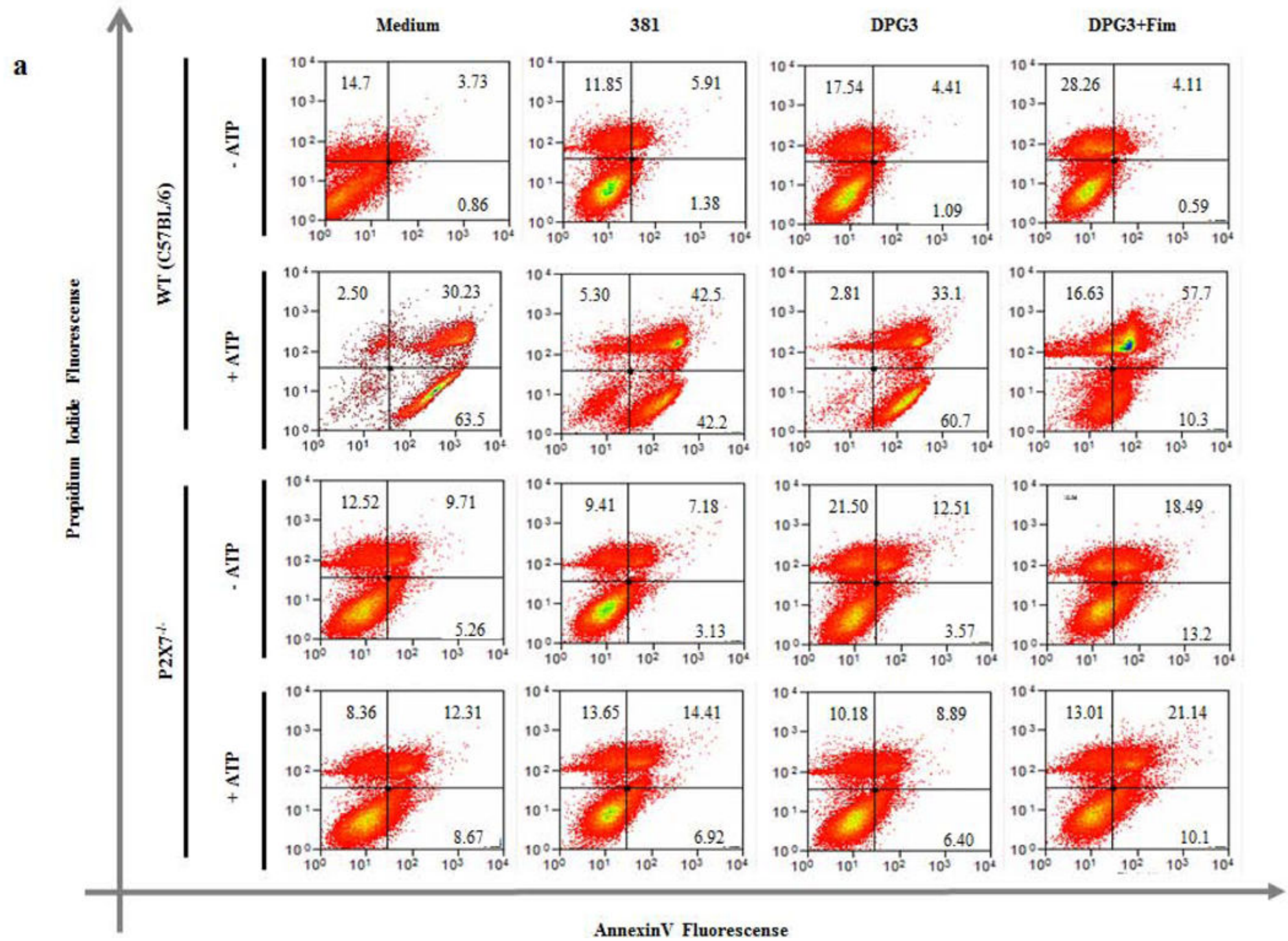
a
Medium
381
DPG3
DPG3+Fim
WT (C57BL/6)
P2X7-/-
- ATP
+ ATP
Propidium Iodide Fluorescense
AnnexinV Fluorescense
14.7
3.73
0.86
11.85
5.91
1.38
17.54
4.41
1.09
28.26
4.11
0.59
2.50
30.23
63.5
5.30
42.5
42.2
2.81
33.1
60.7
16.63
57.7
10.3
12.52
9.71
5.26
9.41
7.18
3.13
21.50
12.51
3.57
18.49
13.2
8.36
12.31
8.67
13.65
14.41
6.92
10.18
8.89
6.40
13.01
21.14
10.1

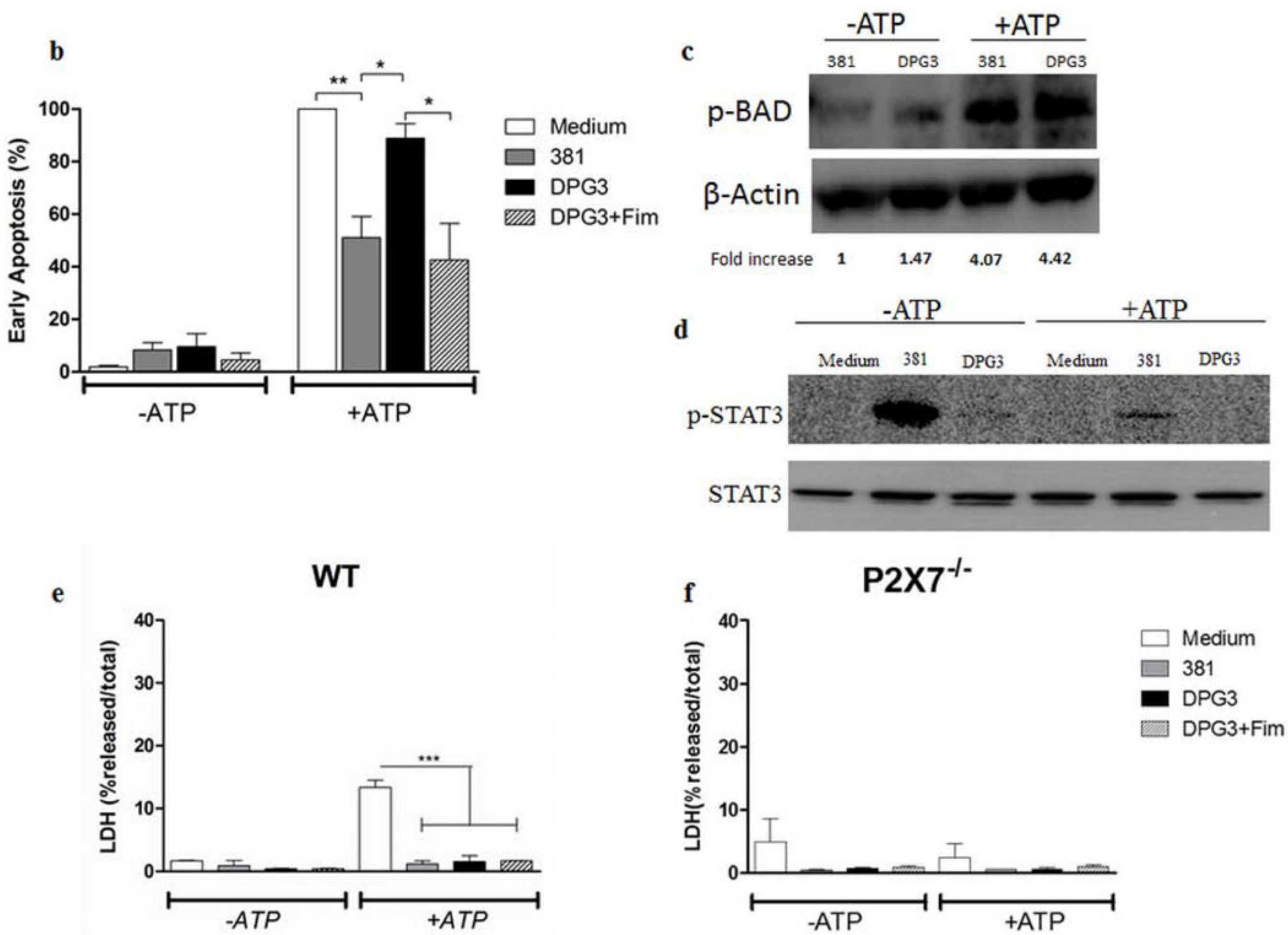

Figure 6. DPG3-stimulated WT cells were more sensitive to early eATP-induced apoptosis through P2X7 receptor

(a) Cell viability was determined by flow cytometry after staining with annexin V and propidium iodide (PI). WT and P2X7$^{-/-}$ BMDMs were harvested with cold PBS after 18 h of infection with *P. gingivalis* strains 381 or DPG3, or DPG3 infection and Fim stimulation (MOI of 100) followed or not by 5 mM eATP incubation for 30 min and stained for annexin V/PI. **(b)** Percentage of early apoptotic cells (Annexin V+/PI−) derived from WT BMDMs after 18 h of infection with *P. gingivalis* strains 381 or DPG3, or DPG3 infection and Fim stimulation (MOI of 100) followed by 5 mM eATP incubation for 30 min and stained for annexin V/PI. The apoptosis values were normalized with respect to the value for Medium +ATP 5mM **(c)** p-BAD and **(d)** p-STAT3/STAT3 expression in WT BMDMs lysates after 18h and 6h, respectively. Cells were infected with *P. gingivalis* strains 381 or DPG3 followed or not by 5mM eATP for 30min where indicated. **(e)** WT and **(f)** P2X7$^{-/-}$ BMDMs were infected for 18 h with *P. gingivalis* strains 381 or DPG3, or stimulated with DPG3 and Fim (MOI of 1:100), followed or not by 5 mM eATP incubation for 30 min, and supernatants were collected for LDH determination. Results are representative of three independent experiments. Asterisk indicates a significant difference compared with indicated treatment group. *p<0.05, **p<0.01.

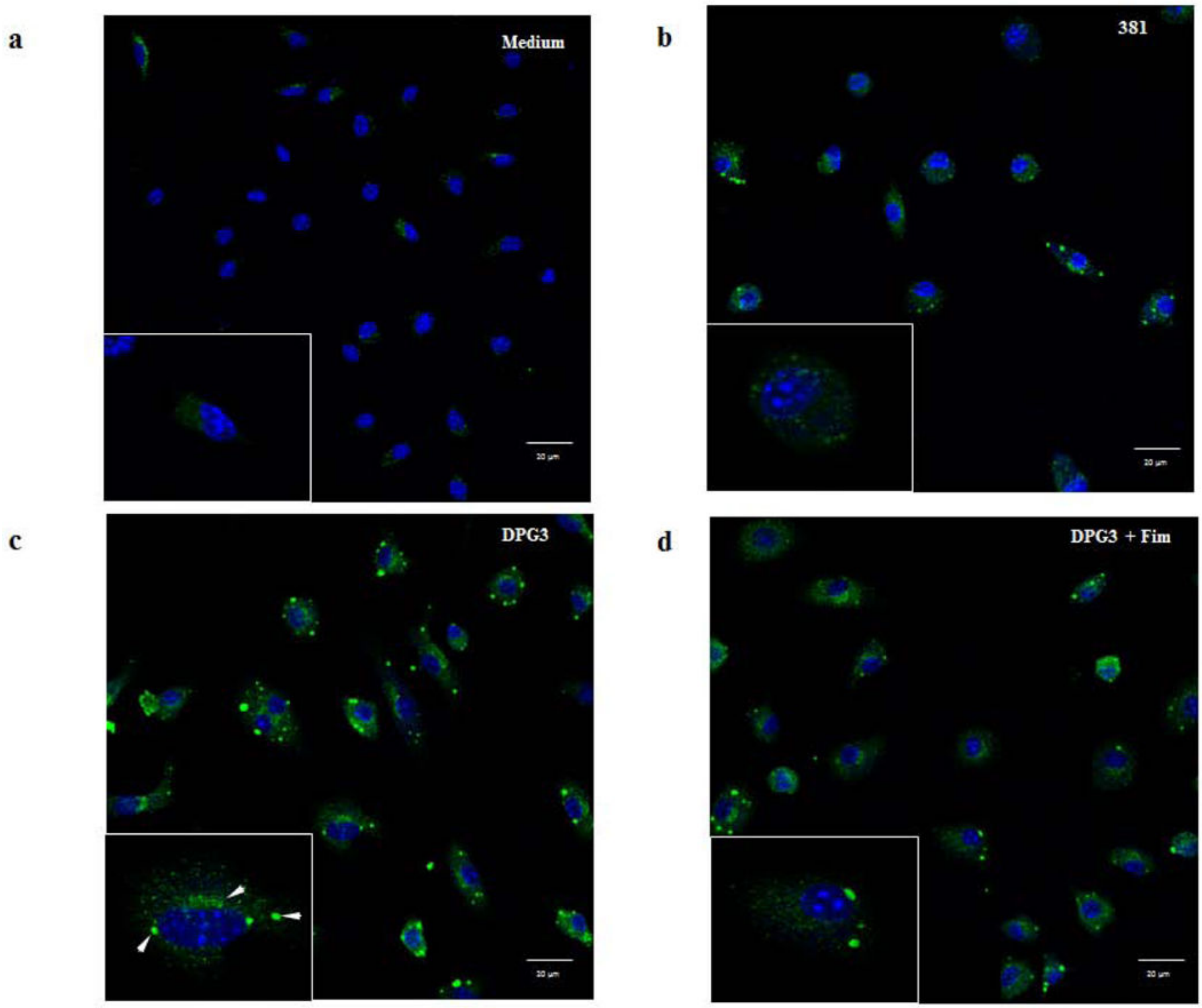

Figure 7. *P. gingivalis* infection modulates P2X7 receptor distribution in a fimbriae-dependent manner

P2X7 receptor expression was analyzed by immunofluorescence and confocal microscopy. Images of foci formation upon *P. gingivalis* infection. BMDMs were grown on glass LabTek chambers and infected for 18h with strains **(b)** 381 or **(c)** DPG3, or **(d)** DPG3+Fim (MOI of 100) as indicated and processed for immunofluorescent staining for P2X7 (green) and mounted on a hard mounting medium containing DAPI (blue). The lower left panel shows one cell at a higher magnification (zoom 6×) and arrowheads point to examples of P2X7 receptor concentration. Scale bars 10 μm. Confocal magnification 63×.